Evaluation and Mitigation of AC Losses in a Fully Superconducting Machine for Wind Turbine Applications

Thanatheepan Balachandran, Dongsu Lee, Noah Salk, Jianqiao Xiao, and Kiruba S. Haran

***Abstract*—A significant challenge in the design of fully superconducting (SC) machines is managing ac losses in the SC armature. Recent developments in MgB_2 superconducting conductors promise low ac loss conductors suitable for fully SC machines. This paper presents an optimized design targeting low losses and low weight for a 10-MW fully SC generator suitable for offshore wind turbine applications. An outer rotor air-core machine topology is investigated to optimize the design with low weight and low losses. An active shielding concept is used to minimize the pole count without adding excessive weight. This enables a reduction in the electrical frequency for a practical design by a factor of 4 to 5 over current designs, driving ac losses and active components weight lower by an order of magnitude. In this study, armature current is varied to control electrical and magnetic loading in order to minimize losses. A pole count study is conducted to identify the design space suitable for MW scale machines. A comparison is made between active shield, passive shield and a hybrid topology to address the benefits of an active shield for weight reduction. Results suggest that low-pole-count designs with MgB_2 conductors will enable machines with less than 1 kW of ac losses.**

***Index Terms*—Electric machines, generators, superconducting coils, wind energy, superconducting machines, superconducting ac loss.**

I. Introduction

OFFSHORE wind turbines are becoming an integral part of future large-scale renewable generation initiatives. It is envisioned that to scale up offshore wind turbines to the range of 10+ MW, superconducting (SC) technologies must be explored. Several partial and fully SC machine designs have been proposed and demonstrated for offshore direct-drive wind turbines. It is theoretically shown that a fully SC topology can improve the efficiency and power density of wind turbines while lowering the levelized cost of energy [1]–[2]. However, before commercial application of fully SC machines, technical complexities must be addressed. A key challenge to be addressed is high ac losses generated in the armature winding. These losses pose a significant barrier for high-speed applications. Due to the low operating frequency of direct-drive wind turbines and the availability of mature, low-loss MgB_2 filaments, it is expected that ac losses will be low enough for practical extraction at cryogenic temperatures.

Most fully SC machines proposed in the literature [3]–[8] are primarily focused on electromagnetic (EM) design and validation of electrical performance; none are optimized for minimal armature ac loss. Practical implementation requires accurate estimations of ac losses and the associated cryogenic design. Therefore, extensive attention must be paid to validating ac loss models and mitigating these losses for a feasible machine design. This paper presents a detailed ac loss evaluation in a 10 MW fully SC machine. An inside-out synchronous generator with MgB_2 race track coils is investigated in this study. A rigorous ac loss calculation along various paths within the armature coils utilizes finite element analysis in tandem with analytical ac loss models available in the literature.

II. Fully Superconducting Machines

Fully SC generators can enable very large (>10 MW) offshore wind turbines which have several economic benefits. Previous design studies conducted on MW-scale fully SC machines show that heat load management in the armature windings is a significant challenge [3]–[8]. These design studies utilize iron yoke or an iron shield which contributes significantly to the weight of the machine. Estimated ac losses in these designs were reported on the order of a kilowatt.

This paper explores a novel high field, air-core fully superconducting machine topology which borrows and adapts a technique utilized in the MRI industry: that of an active magnetic shield comprised of SC coils to contain the flux within the machine [9]–[11]. This topology enables low-pole-count designs that minimize weight by eliminating additional iron. Fig. 1 illustrates the basic design concept and the main features of a completely air-core synchronous machine. The proposed machine specifications are given in Table I. In this study, the MgB_2 conductor data provided in Table II is chosen for both the armature and field coils.

III. Estimating AC Losses

In a fully SC generator, the armature coils will carry time-varying current while being exposed to a rotating magnetic field with some phase delay. These conditions will generate heat within the SC armature coils, a phenomenon known as ac loss. These losses are cyclical and increase with both applied frequency and peak applied flux density squared. Even though, wind turbines operate at low speeds and therefore experience low

Manuscript received September 25, 2019; accepted March 30, 2020. Date of publication April 13, 2020; date of current version May 28, 2020. This work was supported by United States National Science Foundation under NSF award no 1807823. *(Corresponding author: Dongsu Lee.)*

The authors are with the Department of Electrical and Computer Engineering, University of Illinois at Urbana Champaign, Urbana, IL 61801 USA (e-mail: dongsul@illinois.edu).

Color versions of one or more of the figures in this article are available online at https://ieeexplore.ieee.org.

Digital Object Identifier 10.1109/TASC.2020.2987015

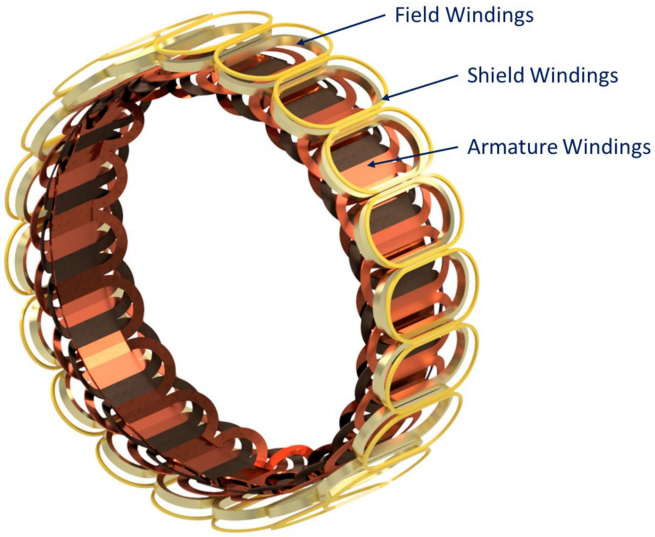

Fig. 1. Arrangement of armature, field and shield SC coils in proposed machine.

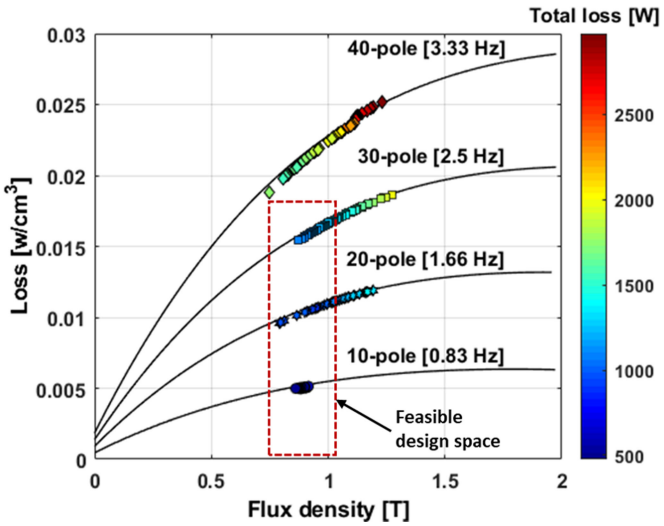

Fig. 2. Design space for 10 MW wind turbine. The feasible design space is marked with red box.

TABLE I
PROPOSED MACHINE SPECIFICATION

Specification	Value
Power	10 [MW]
Number of phases	3
Speed	10 [rpm]
Air-gap length	80 [mm]
Outer diameter	max 4.4 [m]
Pole number	10, 20, 30, 40
Superconductor	MgB_2
Operating temperature	20 [K]
Rated line to line voltage	6.6 [kV_{rms}]
Armature slots per pole	6 (3-ϕ per pole)
Number of parallel connection	4
Armature current density	max 200 [A_{rms}/mm^2]
Field current density	200 [A/mm^2]
Shield current density	200 [A/mm^2]

TABLE II
MgB_2 CONDUCTOR DATA ($D_0 = 0.32/d_f = 10/L = 5$) [MM/$\mu$M/MM] [13]
SUPPLIER: HYPER TECH RESEARCH

Parameter	Symbol	Value
Critical current density at 20 K and self field 2 T [A/mm^2]	J_c	1780
SC outer diameter [mm]	D_o	0.32
Filament diameter [mm]	d_f	0.01
Number of filaments	n	114
SC fill factor	λ	0.15
Effective fill factor	λ_e	0.49
Transverse resistivity [Ω-mm]	ρ	$3.65E^{-4}$
Effective transverse resistivity [Ω-mm]	ρ_e	$1.25E^{-4}$
Twist pitch [mm]	L	5

electrical frequencies, accumulated losses in the large armature coils are significant and determine the feasibility of a design. In this paper, Carr's model [12] is used to estimate losses in the armature windings. Losses are evaluated across a unit length of wire and integrated over the total volume to compute the total loss. This model is widely used and was tweaked to estimate the losses in [13] for MgB_2 conductors and YBCO tapes as well as experimentally validated for low field and low frequency conditions [14].

With μ_0, J_c, and d_f denoting the magnetic permeability, critical current density, and filament diameter respectively, the following equations are used to compute hysteresis (P_h), eddy current (P_e), coupling (P_c), and transport current (P_t) losses with an applied peak flux density, B_m.

$$P_h = \frac{4}{3} J_c d_f B_m f \lambda \tag{1}$$

$$P_e = \frac{\pi^2}{k\rho_e}(D_o B_m f)^2 \tag{2}$$

$$P_c = \frac{1}{n\rho_e}(L B_m f)^2 \tag{3}$$

$$P_t = \frac{\mu_0 f}{\pi} I_c^2 \frac{\left[(1-\frac{I_0}{I_c})\ln(1-\frac{I_0}{I_c}) + \frac{I_0}{I_c} - 0.5(\frac{I_0}{I_c})^2\right]}{\pi(\frac{D_o}{2})^2} \tag{4}$$

where $I_0, I_c, f, \lambda, \rho_e, L$, and D_0 are the operating current, critical current, applied frequency, fill factor, copper matrix effective transverse resistivity, twist pitch, and SC outer diameter respectively. The constants n and k are set to be 2 and 4 respectively as required for circular, multi-filament SC wires [13]. When comparing each loss component between 0 and 2 T, due to the low frequency and high field, hysteresis losses dominate in this wind turbine design space. The solid lines in Fig. 2 show the projected total loss per cm^3 variation with flux density between 0 to 2 T, assuming the operating current is 50% of the critical current at the applied field. This provides a safety margin to

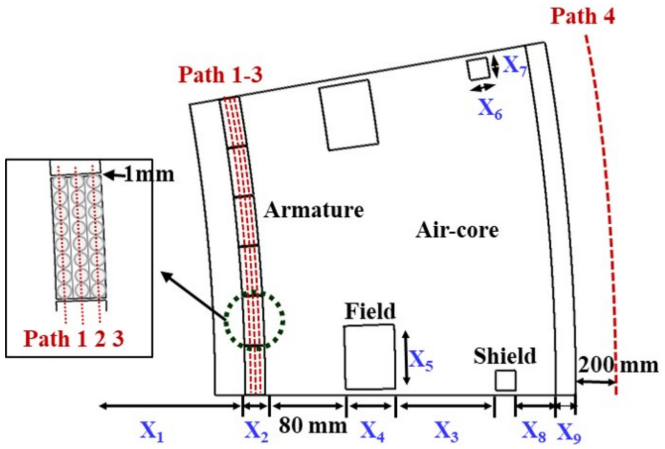

Fig. 3. Design variables of the machine (reproduced from [11]).

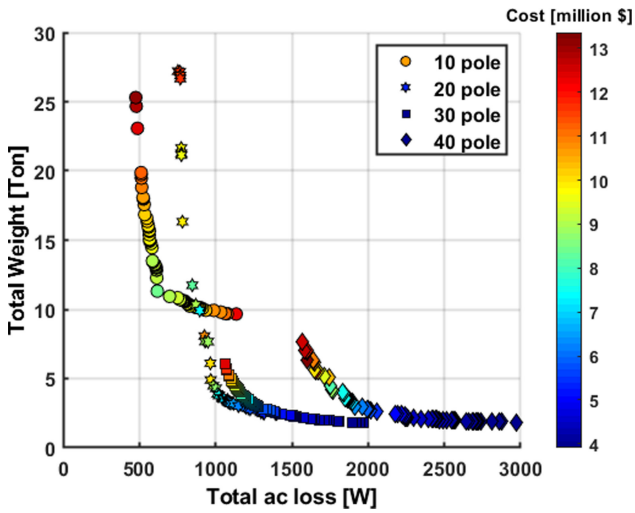

Fig. 4. Optimal Pareto-front of various pole count machines.

TABLE III
DESIGN SPACE BOUNDARIES

Parameter	Minimum	Maximum
Armature slot inner radius (X_1) [mm]	1500	2000
Armature slot radial height (X_2) [mm]	1	100
Radial distance between field coils and shield coils (X_3) [mm]	1	100
Field slot radial height (X_4) [mm]	1	100
Field slot circumferential width (X_5) [degrees]	1	*f(# poles)*
Shield slot radial height (X_6) [mm]	0.5	100
Shield slot circumferential width (X_7) [mm]	0.5	*f(# poles)*
Radial distance between shield coil and iron shield (X_8) [mm]	1	100
Radial iron shield height (X_9) [mm]	1	100
Armature current density (X_{10}) [A/mm^2]	50	200

account for hot spots and other non-idealities in the conductor [15]. Each point in the scatter plot in Fig. 2 corresponds to a 10 MW machine design obtained from the optimization results. Non-feasible designs are eliminated during the optimization via a fitness function and no design outside of 0.8 T to 1.2 T air-gap field survived the genetic algorithm. As can be seen from Fig. 2, when the flux density goes below 0.8 T, the designs become heavy. On the other hand, when the flux density goes above 1.2 T, total losses become significant.

IV. Optimization Scheme

A genetic algorithm (GA) based optimization tool, GOSET, [17] is used to optimize the machine for minimal weight and ac losses. Machine design variables and ranges are provided in Fig. 3 and Table III respectively. Design variables generated from the GA are passed to a finite element analysis (FEA) tool, Altair Flux, to perform the 2-D static EM analysis of each generator. In the FEA tool, SC windings are modeled as equivalent conventional conductors with large current densities to evaluate the machine EM performance. Then the EM results are utilized in analytical models to estimate ac losses, cost, and weight of the machine. These results are fed back to the GA tool for fitness evaluation and synthesis of a new generation.

The armature current density is set as a free variable to allow the optimization of both electrical and magnetic loading. Depending on the air-gap field, the armature critical current is evaluated using a polynomial fit extrapolated from J_c vs B data provided by Hyper Tech Research; similar data is also used in [14]. The optimization verifies that the operating current is below 50% of the critical current at the applied field. The cost of MgB_2 conductors is estimated from price information provided by Hyper Tech Research. Given a price of \$10/m for a 0.83 mm diameter strand, the cost of a similar 0.32 mm diameter strand is estimated as \$1.5/m. Iron cost is assumed to be \$2/kg.

V. Results

A Pareto-optimal front for the entire design space is shown in Fig. 4. Every design in the Pareto-front is a 10 MW machine satisfying the diameter (<4.4 m), axial length (<5 m), critical current density safety margin, and external flux density constraints (<50 mT). From the results, a clear trade-off between weight and ac losses is evident. Pole count significantly impacts weight, ac losses and SC usage. As the pole count increases, machine weight decreases, and ac losses increase. Higher pole counts result in lower minimum weight designs; however, the minimum weight is achieved at the expense of higher losses.

A Pareto-optimal front for a 10-pole machine is given in Fig. 5. This shows the impact of an iron shield on overall weight. Designs with significant iron shield tend to have low losses and higher weight. Optimal results converge toward a hybrid design which has a combination of iron shield and active shield. A comparison of machine parameters for a 10-pole design is given in Table IV. The flux density distribution of the optimal machine design is given in Fig. 6 and a corresponding mechanical design is shown in Fig. 7. Results show that a 10-pole machine with 618 W ac losses is possible with an axial length of 2.45 m and a diameter of 4.29 m. Using cryocooler weight and efficiency data obtained from a survey conducted on commercially available cryocoolers [16] on Page 27 in Table 6, the following assumptions are used to estimate the system weight and efficiency:

- Reverse-Brayton cryocooler efficiency is 2% at 20 K.
- Marginal increase in cryocooler weight to remove 1 W of heat load is 1 kg at output power >100 W (from Fig. 8).
- Additional machine component weight is estimated from a 3D CAD model of the machine shown in Fig. 7.

Required cryocooler power, machine efficiency considering ac loss as well required cryogenic power, and weight for the best

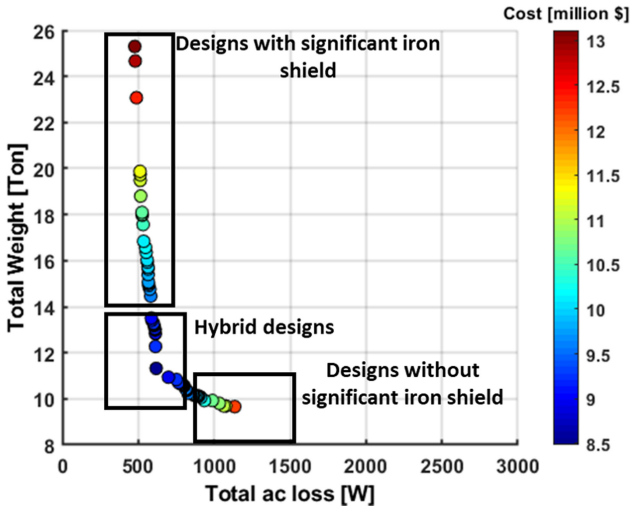

Fig. 5. Optimal Pareto front of 10-pole machine.

TABLE IV
COMPARISON OF MACHINE DESIGNS - 10 POLE

Parameter	Best Weight Design	Best AC Loss Design	Best Overall Design
Outer diameter [m]	4.18	4.34	4.29
Axial length [m]	3.34	4.72	2.45
Air-gap flux density [T]	0.88	0.86	0.91
Outside flux density [T]	0.049	0.048	0.044
Armature SC length [km]	2852	1190	1494
Field SC length [km]	3316	4850	2610
Shield SC length [km]	1656	2683	1544
Total SC length [km]	8125	7917	5648
Iron shield weight [Ton]	4.27	19.51	7.57
Total loss [W]	1135	477	618
Weight (iron and SC) [Ton]	9.7	25.3	11.4
Cost (iron and SC) [million$]	12.1	13.1	8.5

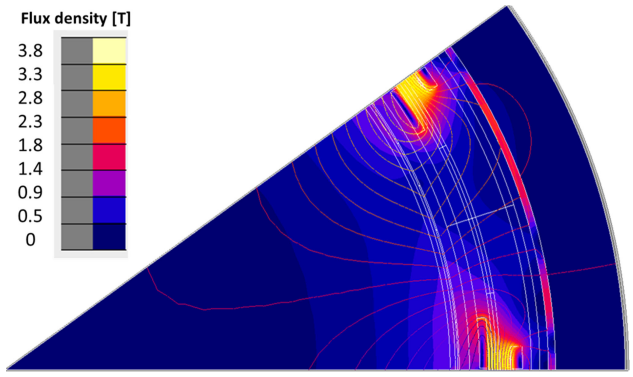

Fig. 6. Flux density distribution of optimal 10-pole machine.

overall design are given by:

$$\underset{\text{Input Power}}{\text{Cryocooler}} = \frac{1}{\underset{\text{Efficiency}}{\text{Cryocooler}}} \cdot \underset{\text{AC Loss}}{\text{Total}} = 30.9 \text{ kW} \quad (5)$$

$$\underset{\text{Efficiency}}{\text{Machine}} = \frac{\underset{\text{Power}}{\text{Rated}} - \left(\underset{\text{Input Power}}{\text{Cryocooler}} + \underset{\text{AC Loss}}{\text{Total}}\right)}{\underset{\text{Power}}{\text{Rated}}} \cdot 100 = 99.68\% \quad (6)$$

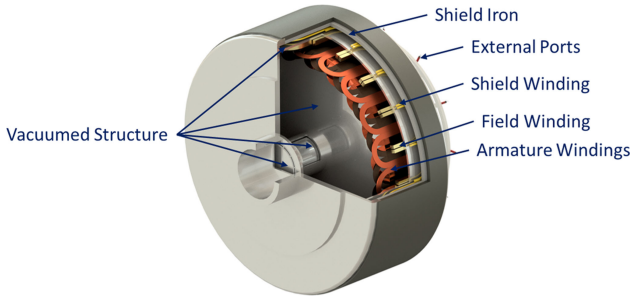

Fig. 7. Mechanical design of the machine with layered vacuum structure.

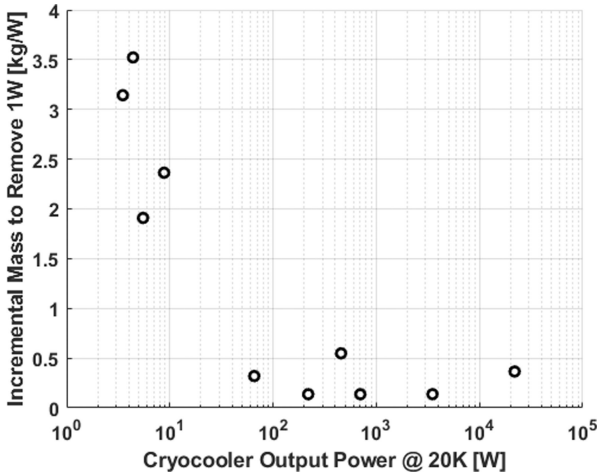

Fig. 8. Commercially available reverse-Brayton cycle cryocooler incremental mass to remove 1 W of heat load @ 20 K, data extracted from [16].

$$\underset{\text{Weight}}{\text{Total}} = \underset{\text{Weight}}{\text{Active}} + \underset{\text{Weight}}{\text{Additional}} + \underset{\text{Weight}}{\text{Marginal}} \cdot \underset{\text{AC Loss}}{\text{Total}} = 40 \text{ Ton} \quad (7)$$

However, it can be noted that low pole count machines tend to have higher active material cost (which is dominated by the amount of SC usage). Considering ac loss, 10-pole machines are an attractive choice, however, when cost and weight are factored in, a trade-ff appears that will be investigated in future studies.

VI. CONCLUSION

Preliminary results show that fully SC machines are attractive for off-shore wind turbine applications. Initial optimization results shows that low pole count machine design with ac losses lower than 1 kW can be achieved. This results in improved efficiency and reduced total system weight. The optimization results highlight a trade-off between ac losses and weight. It is identified that the feasible air-gap field limits for a 10 MW fully SC wind generator is within 0.8 T and 1.2 T. Results show that an iron shield adds weight and reduces ac losses in the machine. The active shield topology enables low-pole-count machine designs without significantly increasing machine weight, resulting in an order of magnitude reduction in weight compared to a conventional iron shield design of the same pole count. This reduction in weight comes without sacrificing the benefit of low ac losses present in low-pole-count machines. It should be noted, however, that the higher SC usage on low-pole-count machines make them more expensive to build. In future studies, minimizing cost will be added as an objective in the optimization to further explore the feasible machine design space for offshore wind turbines.

REFERENCES

[1] T. Hoang, L. Quval, C. Berriaud, and L. Vido, "Design of a 20-MW fully superconducting wind turbine generator to minimize the levelized cost of energy," *IEEE Trans. Appl. Supercond.*, vol. 28, no. 4, Jun. 2018, Art no. 5206705.

[2] A. B. Abrahamsen *et al.*, "Comparison of levelized cost of energy of superconducting direct drive generators for a 10-MW offshore wind turbine," *IEEE Trans. Appl. Supercond.*, vol. 28, no. 4, Jun. 2018, Art. no. 5208205.

[3] S. S. Kalsi, "Superconducting wind turbine generator employing MgB_2 windings both on rotor and stator," *IEEE Trans. Appl. Supercond.*, vol. 24, no. 1, Feb. 2014, Art. no. 5201907.

[4] A. B. Abrahamsen, N. Magnusson, D. Liu, E. Stehouwer, B. Hendriks, and H. Polinder, "Design study of a 10 MW MgB_2 superconductor direct drive wind turbine generator," in *Proc. Eur. Wind Energy Assoc.*, 2014, pp. 1–7.

[5] F. Lin, R. Qu, D. Li, Y. Cheng, and J. Sun, "Electromagnetic design of 13.2 MW fully superconducting machine," *IEEE Trans. Appl. Supercond.*, vol. 28, no. 3, Apr. 2018, Art. no. 5205905.

[6] M. Saruwatari *et al.*, "Design study of 15-MW fully superconducting generators for offshore wind turbine," *IEEE Trans. Appl. Supercond.*, vol. 26, no. 4, Jun. 2016, Art. no. 5206805.

[7] Y. Terao, M. Sekino, and H. Ohsaki, "Electromagnetic design of 10 MW class fully superconducting wind turbine generators," *IEEE Trans. Appl. Supercond.*, vol. 22, no. 3, Jun. 2012, Art. no. 5201904.

[8] Y. Liang, M. D. Rotaru, and J. K. Sykulski, "Electromagnetic simulations of a fully superconducting 10-MW-class wind turbine generator," *IEEE Trans. Appl. Supercond.*, vol. 23, no. 6, Dec. 2013, Art. no. 5202805.

[9] K. S. Haran, D. Loder, T. O. Deppen, and L. Zheng, "Actively shielded high-field air-core superconducting machines," *IEEE Trans. Appl. Supercond.*, vol. 26, no. 2, Mar. 2016, Art. no. 5202508.

[10] D. Lee, T. Balachandran, H. Cho, and K. Haran, "Exploring fully superconducting air-core machine topology for off-shore wind turbine applications," *IEEE Trans. Magn.*, vol. 55, no. 7, Jul. 2019, Art. no. 8106506.

[11] T. Balachandran, D. Lee, and K. S. Haran, "Optimal design of a fully superconducting machine for 10-MW offshore wind turbines," in *Proc. IEEE Int. Elect. Mach. Drives Conf.*, 2019, pp. 1903-1909.

[12] W. J. Carr, *2001 AC Loss and Macroscopic Theory of Superconductors*. 2nd ed., New York, NY, USA: Taylor and Francis, 2001.

[13] M. D. Sumption, "AC loss of superconducting materials for very high density motors and generators of hybrid-electric aircraft," in *Proc. AIAA/IEEE Elect. Aircraft Technologies Symp.*, 2018, pp. 1–6.

[14] M. D. Sumption, "AC Loss of Superconducting Materials- refined loss estimates for very high density motors and generators for hybrid-electric aircraft: MgB_2 wires, coated conductor tapes and wires," *AIAA Propulsion Energy Forum*, Indianapolis, IN, USA, Aug. 2019.

[15] D. C. Loder and K. S. Haran, "Multi-objective optimization of an actively shielded superconducting field winding pole count study," in *Proc. IEEE Int. Elect. Mach. Drives Conf.*, 2015, pp. 1709–1714.

[16] K. S. Haran *et al.*, "High power density superconducting rotating machines development status and technology roadmap," *Supercond. Sci. Technol.*, vol. 30, 2017, Art. no. 123002.

[17] S. D. Sudhoff, *Optimization-Based Design in Power Magnetic Devices: A Multi-Objective Design Approach*. Hoboken, NJ, USA: Wiley, 2014.